

# 14

## Wilms' Tumor

Sue C. Kaste and Jeffrey S. Dome

The clinical applications of fluorine-18 fluorodeoxyglucose–positron emission tomography ( $^{18}\text{F}$ -FDG-PET) imaging in adults have grown rapidly. However, only recently has this technology and the merged technology of PET and computed tomography (PET-CT) been extended to children and adolescents. Thus, information about the indications and utility of PET-CT in pediatric oncology is limited. This chapter discusses the initial experience with PET and PET-CT imaging of patients with Wilms' tumor.

### Epidemiology of Wilms' Tumor

Wilms' tumor is the most common malignant pediatric renal tumor and accounts for 6% of all cases of childhood cancer in the United States each year. Approximately eight cases are identified annually per million children under the age of 15 years; the annual number of new cases in the United States is estimated to be 500 (1). The frequency of Wilms' tumor is slightly higher in blacks than in whites but is considerably lower in Asians than in whites. In the United States, the incidence of Wilms' tumor (either unilateral or bilateral) is slightly less in boys than in girls (2).

The association between Wilms' tumor and genetic malformation syndromes is well known, although these syndromes are present in only a small number of patients with Wilms' tumor. The syndromes most commonly associated with Wilms' tumor are WAGR (Wilms' tumor, *aniridia*, genitourinary malformation, mental retardation) syndrome, Denys-Drash syndrome (pseudohermaphroditism, glomerulopathy, renal failure, and Wilms' tumor), and Beckwith-Wiedemann syndrome (macroglossia, omphalocele, visceromegaly, hemihypertrophy, Wilms' tumor, and other cancers) (3).

### Pathology

Classical Wilms' tumor contains blastemal, epithelial, and stromal cells, although many tumors do not contain all three types of cells (4). About 7% of tumors contain anaplasia, which is defined by cells with enlarged

nuclei, hyperchromasia, and irregular mitotic figures (5). When present, anaplasia usually occurs diffusely throughout a tumor but also may be focal (6). Patients whose tumors contain focal anaplasia have better outcomes than those whose tumors contain diffuse anaplasia (7). Tumors that are not anaplastic at all are associated with the best prognosis and are thus designated as having “favorable histology.” Less common renal tumors of childhood include clear cell sarcoma of the kidney, malignant rhabdoid tumor, congenital mesoblastic nephroma, and renal cell carcinoma.

Nephrogenic rests are precursors of Wilms’ tumor; these are clusters of embryonal nephroblastic cells that persist abnormally into childhood (8). Nephrogenic rests are found in about 40% of patients with unilateral Wilms’ tumor and in nearly all patients with bilateral Wilms’ tumor (8). Nephrogenic rests are classified as nascent/dormant, maturing/sclerosing, or hyperplastic. Hyperplastic nephrogenic rests can be quite large and are often difficult to distinguish from Wilms’ tumor (8).

## Prognostic Factors

The most powerful prognostic factors for patients with Wilms’ tumor are tumor histology and stage. Anaplastic histology predicts a markedly higher risk of recurrence than does favorable histology. Likewise, advanced tumor stage is associated with increased risk of recurrence. Other adverse prognostic factors include older patient age (9,10), blastemal-predominant histology after chemotherapy (11), loss of heterozygosity on chromosome arms 1p and 16q (12,13), gain of chromosome arm 1q (14), and a high level of telomerase expression (15,16). Ongoing biology studies are likely to identify additional molecular prognostic factors.

## Treatment

The treatment of Wilms’ tumor involves surgery, chemotherapy, and, in some cases, radiation therapy. The longstanding approach used by the National Wilms’ Tumor Study Group (NWTSG) has been a nephrectomy at the time of diagnosis, with subsequent chemotherapy and radiation therapy (17). The approach used by the International Society of Pediatric Oncology (SIOP) has been to administer several weeks of chemotherapy before nephrectomy (18). Each approach has distinct advantages, and the outcomes are similar. Table 14.1 lists the outcomes of patients treated on the most recently reported NWTSG studies. Given the excellent overall survival rates of patients with Wilms’ tumor, a priority of recent clinical trials has been to limit therapy, and its associated toxicity, in patients who are at low risk of disease recurrence.

**Table 14.1. Outcomes of patients treated on the National Wilms' Tumor Study Group (NWTSG) studies NWTSG-3 and -4 (Data from 7, 19)**

Tumor histology and stage	4-Year relapse-free survival (%)	4-Year overall survival (%)
<b>Favorable histology</b>		
Stage I	89.0	95.6
II	87.4	91.1
III	82.0	90.9
IV	79.0	80.9
V (bilateral)	–	81.7
<b>Diffuse anaplasia</b>		
Stage I	93.8	93.3
II	71.6	70.1
III	58.7	56.3
IV	16.7	16.7

## Potential Applications of PET/PET-CT Imaging to Wilms' Tumor

Functional imaging studies such as PET or PET-CT may increase the accuracy of tumor staging, distinguish between benign and malignant lesions, and assess the early response to treatment in patients with measurable tumors. Although experience with  $^{18}\text{F}$ -FDG-PET/PET-CT imaging in Wilms' tumor is limited, preliminary reports (20) and our experience suggest that Wilms' tumors are often  $^{18}\text{F}$ -FDG-avid.

### Tumor Staging

Diagnostic imaging studies play a key role in the staging of primary Wilms' tumor. Imaging studies delineate the local extent of the tumor and detect the presence of metastatic disease (Fig. 14.1). The most common sites of metastasis are the lungs, regional lymph nodes, and liver. Approximately 10% of patients have lung metastases at diagnosis (21), and 47% have pulmonary metastases at the time of relapse (22).

Chest radiography and chest CT are routinely used to detect pulmonary metastatic disease (23,24). Chest radiographs are limited by resolution and sensitivity; CT imaging is complicated by inter- and intraobserver discordance in interpreting the presence and significance of pulmonary nodules (25). A common dilemma faced by clinicians is the management of patients with small pulmonary nodules. The NWTSG reported that 17% of lung nodules in patients with newly diagnosed Wilms' tumor were found on biopsy to be benign (26). Therefore, the management of such lesions is particularly problematic unless biopsy is performed. Although several studies have shown an increased risk of pulmonary relapse in patients with CT-identified pulmonary nodules, intensified chemotherapy and pulmonary irradiation are not without toxic effects (25–27). As with other pediatric malignancies, pulmonary metastases of Wilms' tumor can differentiate into benign mature tumor cells, further complicating the interpretation of

follow-up imaging examinations on the basis of anatomic appearance (27–29).

$^{18}\text{F}$ -FDG has the potential ability to differentiate metabolically hyperactive nodules from quiescent and metabolically hypoactive nodules (30,31). Because both malignant and inflammatory diseases can involve glucose hypermetabolism,  $^{18}\text{F}$ -FDG-PET/PET-CT is unlikely to differentiate benign from malignant nodules with absolute specificity. However, with refinement of PET techniques, including quantitative techniques and delayed imaging, characteristics that differentiate benign from malignant lesions may be discerned. Even with the currently available techniques, hypermetabolic pulmonary lesions would be more likely to be malignant and therefore could be preferentially biopsied.

Accurate staging of recurrent Wilms' tumor facilitates the design of multidisciplinary regimens to treat all sites of disease.  $^{18}\text{F}$ -FDG-PET/PET-CT provides sensitive detection of metabolically active sites of disease, some of which are undetected by other imaging modalities (Fig. 14.2). A patient treated for recurrent anaplastic Wilms' tumor at St. Jude Children's Research Hospital, Memphis, TN, had persistent pulmonary nodules in the right middle lobe after chemotherapy. Surgical removal of the affected area of the lung was considered, and a PET-CT scan was performed to detect other possible sites of disease. The PET-CT scan revealed FDG avidity in the right pulmonary hilum

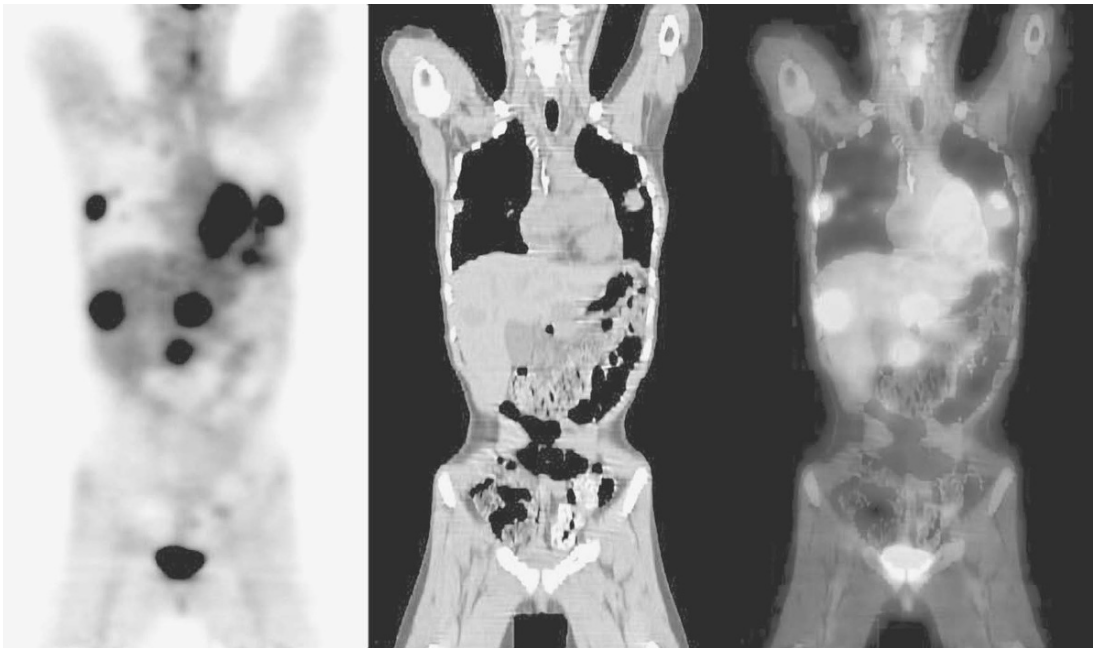


**Figure 14.1.** Fluorine-18 fluorodeoxyglucose–positron emission tomography ( $^{18}\text{F}$ -FDG-PET)–computed tomography (CT) images of a 10-year-old girl with recurrent Wilms' tumor. PET-CT imaging was performed to determine the extent of disease. Note numerous sites of  $^{18}\text{F}$ -FDG avidity. (Courtesy of Dr. Barry Shulkin.)

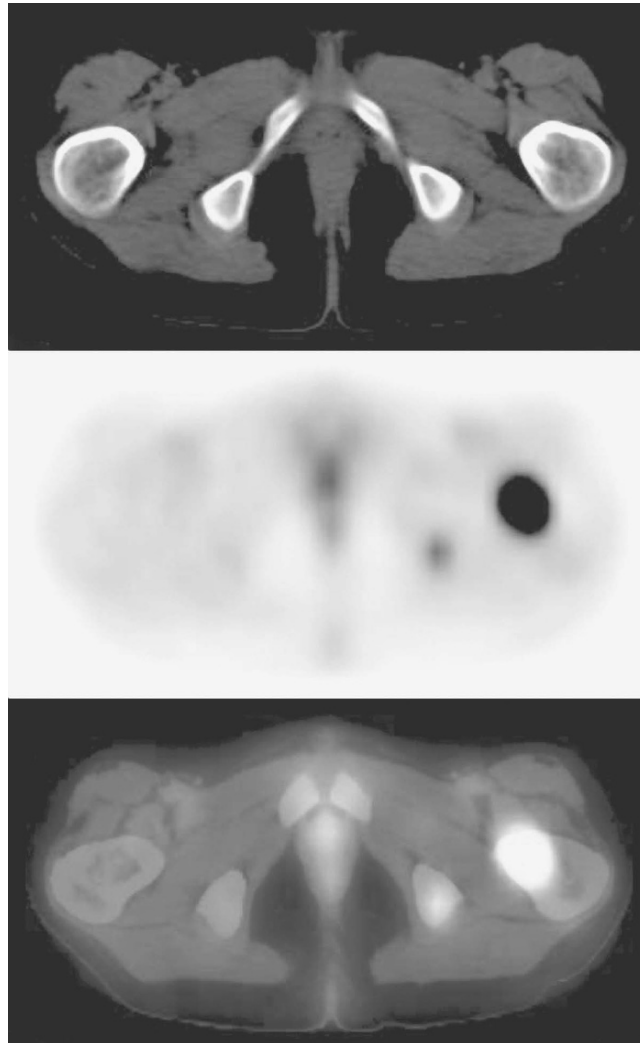


**Figure 14.2.** Intensely  $^{18}\text{F}$ -FDG-avid lesions in the left proximal femur and ischium of this patient (also shown in Fig. 14.1) were not evident on the corresponding CT images captured with bone windows. (Courtesy of Dr. Barry Shulkin.)

and upper right chest, suggesting that the tumor was widespread and that complete resection would be impossible (Fig. 14.3).

### **Bilateral Wilms' Tumor**

The treatment of bilateral Wilms' tumor is challenging. The goal of treatment is to eradicate tumor cells while preserving as much renal parenchyma as possible. Patients typically receive preoperative chemotherapy, thereby reducing tumor burden and facilitating surgery. Approximately 40% of tumors are reduced more than 50% in size by

chemotherapy (32). Failure to respond can signify that the tumor cells are anaplastic or otherwise resistant to treatment, requiring augmentation of therapy and perhaps nephrectomy. However, tumors with extensive rhabdomyomatous differentiation or necrosis may also fail to respond, and augmentation of chemotherapy is not indicated for these cases. Positron emission tomography scanning has been reported to differentiate viable germ cell tumor from mature teratoma and tissue necrosis (33), and therefore it may also help in distinguishing between proliferating and nonproliferating bilateral Wilms' tumor.

A theoretical obstacle to the use of PET scanning to image bilateral Wilms' tumor is the possibility that clearance of  $^{18}\text{F}$ -FDG through the genitourinary tract could mask an intrarenal tumor. However, active tumors can be visualized within the renal parenchyma due to

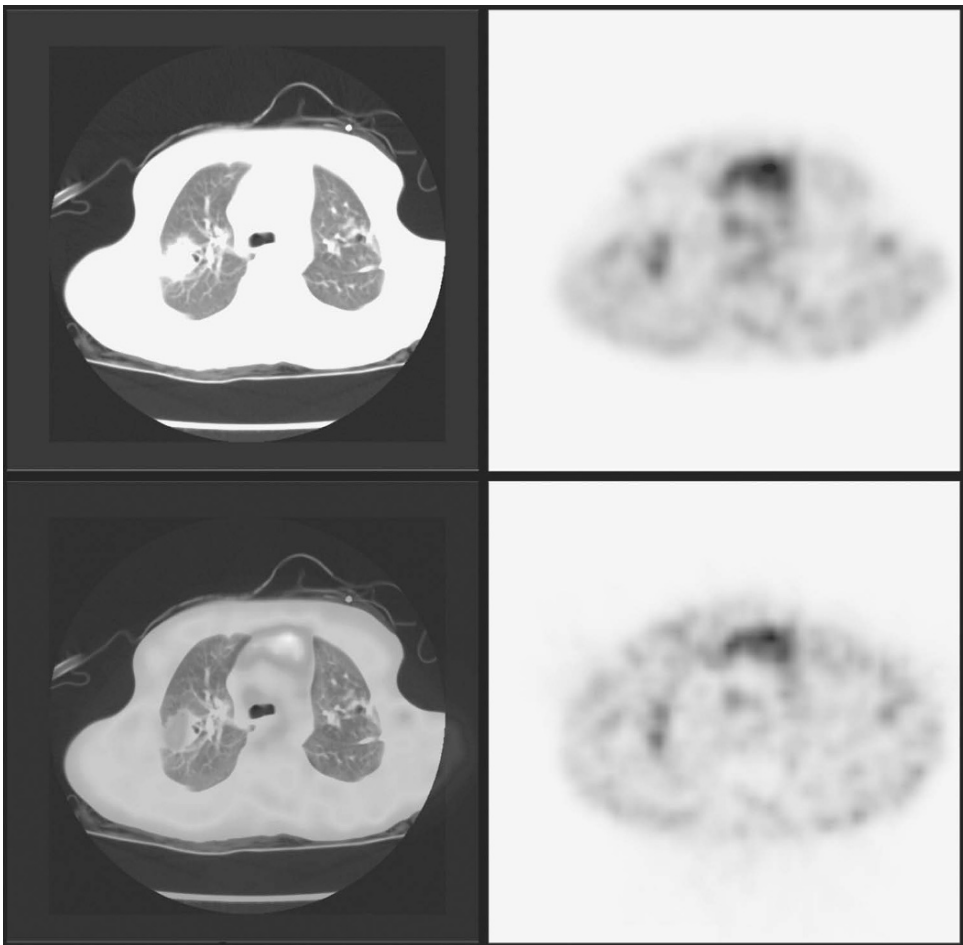


**Figure 14.3.** A patient treated for recurrent anaplastic Wilms' tumor underwent PET-CT imaging to detect other possible sites of disease before undergoing a possible right middle lobectomy for pulmonary nodules that persisted after chemotherapy.  $^{18}\text{F}$ -FDG avidity in the right pulmonary hilum and upper right chest indicated widespread metastatic disease that precluded complete resection.

higher uptake by tumor than by normal kidney (20,34). Shulkin and colleagues (20) reported two patients with bilateral Wilms' tumor who underwent PET scans to guide clinical management. One patient with bilateral multifocal Wilms' tumor had an initial response to therapy during the first 2 months of treatment, but then had stable disease. A PET scan showed persistent  $^{18}\text{F}$ -FDG avidity in one of the right-kidney tumors, which was confirmed by biopsy to be Wilms' tumor. Interestingly, the left kidney, which was not FDG-avid, also contained Wilms' tumor with areas of nephroblastomatosis. It would be informative to know whether the difference in FDG avidity reflected residual Wilms' tumor in the right kidney that was less differentiated and proliferative than that in the left kidney.

The second patient underwent bilateral open biopsy of bilateral renal masses that showed favorable-histology Wilms' tumor in the right kidney and anaplastic Wilms' tumor in the left kidney. She underwent  $^{18}\text{F}$ -FDG imaging after the left renal mass failed to decrease in size to the same extent as the right renal mass in response to chemotherapy. The PET scan revealed  $^{18}\text{F}$ -FDG avidity in the rim of the left renal mass but no uptake in the right renal mass. Bilateral partial nephrectomy revealed residual viable tumor in the left kidney but necrotic tumor without viable elements on the right side, correlating well with the PET findings (20). A systematic study of PET scans in patients with bilateral Wilms' tumor is warranted to assess whether the level of  $^{18}\text{F}$ -FDG activity correlates with histologic response to therapy.

### **Differentiating Between Nephrogenic Rests and Wilms' Tumor**

The difficulty of distinguishing nephrogenic rests and nephroblastomatosis from Wilms' tumor can create a diagnostic dilemma. Although the two entities—and the spectrum between them—have some distinct features, their imaging characteristics can be similar. Typically, nephrogenic rests and nephroblastomatosis are multifocal or diffuse bilateral lesions located in the subcapsular portion of the kidneys. They may be classified by their location as intralobar and perilobar, with perilobar nephrogenic rests being more common. On ultrasonography (US) and CT, nephrogenic rests appear as homogeneous, hypodense, poorly enhancing peripheral nodules. As with Wilms' tumor, they are hypointense on T1- and hyperintense on T2-weighted sequences (35). A Wilms' tumor is a hypervascular intrarenal mass that is usually large and may be associated with vascular invasion. Unlike nephrogenic rests, Wilms' tumor is usually an inhomogeneous echogenic solid mass on ultrasound and CT (particularly contrast-enhanced CT) studies. On magnetic resonance imaging (MRI), Wilms' tumor is hypointense on T1- and hyperintense on T2-weighted sequences (35) and enhances inhomogeneously when intravenous contrast medium is used (36–38). Contrast-enhanced MRI improves the imaging distinction of Wilms' tumor from nephrogenic rests, achieving an overall sensitivity of 57% for detection of the lesion and an overall accuracy of 65%. Although better than those of excretory urography and ultrasound, these values are far from ideal. Further, small nephrogenic rests less than 4 mm in

size and those intermixed with Wilms' tumor may be overlooked by MRI (36). Rohrschneider et al. (39) found that the homogeneity of nephrogenic rests is the imaging feature that best differentiates them from Wilms' tumor. The authors also reported US to be less sensitive than CT or MRI in detecting small nephrogenic rests.

$^{18}\text{F}$ -FDG-PET/PET-CT imaging has the potential to distinguish between benign nephrogenic rests and nephroblastomatosis and to identify their potential evolution into Wilms' tumor. Shulkin et al. (20) described a case in which FDG uptake was observed in active sites of Wilms' tumor but absent in benign nephrogenic rests. It is likely that FDG avidity varies according to the subtype of nephrogenic rest (sclerotic vs. hyperplastic). Lesions smaller than 4 or 5 mm might still be overlooked because of the limitations of PET/PET-CT resolution, unless they are very hypermetabolic. It would be worthwhile to prospectively compare  $^{18}\text{F}$ -FDG avidity with histology in patients with bilateral or multifocal kidney lesions.

### Differentiation of Residual Tumor from Other Entities

Residual imaging abnormalities observed after treatment of unresectable or metastatic Wilms' tumor may not indicate viable tumor. It can be difficult to distinguish active or recurrent disease from nonmalignant abnormalities such as postoperative changes, scarring, or abscess formation. Although  $^{18}\text{F}$ -FDG avidity is not a specific indicator of malignancy, increased avidity can identify a site of potential residual or recurrent disease and direct biopsy to the area (20). Figure 14.4 illustrates this application. It shows the PET-CT scan of a patient with stage IV Wilms' tumor with favorable histology who presented with very extensive lung disease. After several months of treatment with

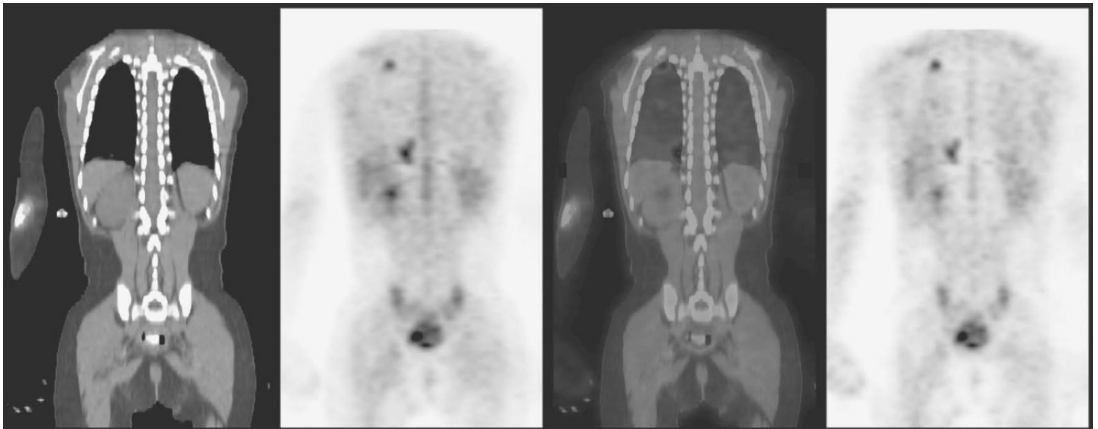


**Figure 14.4.** A young boy who had experienced multiple recurrences of Wilms' tumor had extensive pulmonary scarring caused by multiple thoracotomies for excision of metastatic tumor. Biopsy of the right upper-lobe mass, directed by  $^{18}\text{F}$ -FDG-avidity, demonstrated Wilms' tumor with rhabdomyomatous differentiation, containing predominant stromal cells and a few glandular elements. Interestingly, the mass was FDG-avid, although it was not actively proliferating. This observation raises the question of whether tumors with rhabdomyomatous differentiation may be FDG-avid.

different chemotherapy agents, the patient had progressive pulmonary disease and received lung radiation and more chemotherapy. Therapy was stopped after several more months, although CT of the chest continued to show multiple lesions, some of which were consistent with scar tissue on biopsy. Six months after the completion of therapy, CT scan showed an increase in the size of a right upper lobe nodule. A PET-CT scan was done to evaluate sites of potentially viable tumor within the markedly abnormal-appearing lungs.  $^{18}\text{F}$ -FDG uptake was observed in the growing right lung nodule and the right pulmonary hilum (Fig. 14.4) but not in other abnormal areas. Computed tomography-guided biopsy of the  $^{18}\text{F}$ -FDG-avid nodule revealed a cellular metastatic Wilms' tumor consisting mostly of mature fibrous stroma.

## Conclusion

Although its application in staging Wilms' tumor and monitoring response to treatment is not yet extensive,  $^{18}\text{F}$ -FDG-PET/PET-CT shows promise for identifying metastatic disease, differentiating benign nephrogenic rests and nephroblastomatosis from Wilms' tumor, directing biopsy sites, and contributing to surgical planning. However, large prospective studies are needed to determine the impact of this modality on staging, assessment of treatment response, and ultimate patient outcome.

## Acknowledgments

The authors thank Ms. Sandra Gaither and Ms. Melissa Mills for manuscript preparation and Ms. Sharon Naron for editing.

## References

1. Ries LAG, Eisner MP, Kosary CL, et al. SEER Cancer Statistics Review, 1975–2000. Bethesda, MD: National Cancer Institute, 2003. [http://seer.cancer.gov/csr/1975\\_2000/index.html](http://seer.cancer.gov/csr/1975_2000/index.html).
2. Breslow N, Olshan A, Beckwith JB, et al. Epidemiology of Wilms tumor. *Med Pediatr Oncol* 1993;21(3):172–181.
3. Dome JS, Coppes MJ. Recent advances in Wilms tumor genetics. *Curr Opin Pediatr* 2002;14(1):5–11.
4. Qualman SJ, Bowen J, Amin MB, et al. Protocol for the examination of specimens from patients with Wilms tumor (nephroblastoma) or other renal tumors of childhood. *Arch Pathol Lab Med* 2003;127(10):1280–1289.
5. Bonadio JF, Storer B, Norkool P, et al. Anaplastic Wilms' tumor: clinical and pathologic studies. *J Clin Oncol* 1985;3(4):513–520.
6. Faria P, Beckwith B, Mishra K, et al. Focal versus diffuse anaplasia in Wilms tumor—new definitions with prognostic significance. *Am J Surg Pathol* 1996;20:909–920.
7. Green DM, Beckwith JB, Breslow NE, et al. Treatment of children with stages II to IV anaplastic Wilms' tumor: a report from the National Wilms' Tumor Study Group. *J Clin Oncol* 1994;12(10):2126–2131.

8. Beckwith JB, Kiviat NB, Bonadio JF. Nephrogenic rests, nephroblastomatosis, and the pathogenesis of Wilms' tumor. *Pediatr Pathol* 1990;10(1-2): 1-36.
9. Breslow N, Sharples K, Beckwith JB, et al. Prognostic factors for Wilms' tumor patients with nonmetastatic disease at diagnosis-results of the third National Wilms' Tumor Study. *Cancer* 1991;68:2345-2353.
10. Pritchard-Jones K, Kelsey A, Vujanic G, et al. Older age is an adverse prognostic factor in stage I, favorable histology Wilms' tumor treated with vincristine monochemotherapy: a study by the United Kingdom Children's Cancer Study Group, Wilms' Tumor Working Group. *J Clin Oncol* 2003; 21(17):3269-3275.
11. Weirich A, Leuschner I, Harms D, et al. Clinical impact of histologic subtypes in localized non-anaplastic nephroblastoma treated according to the trial and study SIOP-9/GPOH. *Ann Oncol* 2001;12(3):311-319.
12. Grundy PE, Telzerow PE, Breslow N, et al. Loss of heterozygosity for chromosomes 16q and 1p in Wilms' tumors predicts an adverse outcome. *Cancer Res* 1994;54(9):2331-2333.
13. Grundy RG, Pritchard J, Scambler P, et al. Loss of heterozygosity on chromosome 16 in sporadic Wilms' tumour. *Br J Cancer* 1998;78(9):1181-1187.
14. Hing S, Lu YJ, Summersgill B, et al. Gain of 1q is associated with adverse outcome in favorable histology Wilms' tumors. *Am J Pathol* 2001;158(2): 393-398.
15. Dome JS, Chung S, Bergemann T, et al. High telomerase reverse transcriptase (*hTERT*) messenger RNA level correlates with tumor recurrence in patients with favorable histology Wilms' tumor. *Cancer Res* 1999;59: 4301-4307.
16. Dome JS, Bockhold CA, Li SM, et al. Telomerase RNA expression as a prognostic marker in patients with favorable histology Wilms tumor. *Proc Am Soc Clin Oncol* 2004;23:799.
17. Grundy PE, Green DM, Coppes MJ, et al. Renal tumors. In: Pizzo PA, Poplack DG, eds. *Principles and Practice of Pediatric Oncology*. Philadelphia: Lippincott Williams & Wilkins, 2002:865-893.
18. Tournade MF, Com-Nougue C, de Kraker J, et al. Optimal duration of preoperative therapy in unilateral and nonmetastatic Wilms' tumor in children older than 6 months: results of the Ninth International Society of Pediatric Oncology Wilms' Tumor Trial and Study. *J Clin Oncol* 2001;19(2):488-500.
19. Green DM, Breslow NE, Beckwith JB, et al. Comparison between single-dose and divided-dose administration of dactinomycin and doxorubicin for patients with Wilms' tumor: a report from the National Wilms' Tumor Study Group. *J Clin Oncol* 1998;16(1):237-245.
20. Shulkin BL, Chang E, Strouse PJ, et al. PET FDG studies of Wilms tumors. *J Pediatr Hematol Oncol* 1997;19(4):334-338.
21. D'Angio GJ, Rosenberg H, Sharples K, et al. Position paper: imaging methods for primary renal tumors of childhood: costs versus benefits [published erratum appears in *Med Pediatr Oncol* 1993;21(9):695]. *Med Pediatr Oncol* 1993;21(3):205-212.
22. D'Angio GJ, Breslow N, Beckwith JB, et al. Treatment of Wilms' tumor. Results of the Third National Wilms' Tumor Study. *Cancer* 1989;64(2): 349-360.
23. Wootton-Gorges SL, Albano EA, Riggs JM, et al. Chest radiography versus chest CT in the evaluation for pulmonary metastases in patients with Wilms' tumor: a retrospective review. *Pediatr Radiol* 2000;30(8):533-537.
24. Owens CM, Veys PA, Pritchard J, et al. Role of chest computed tomography at diagnosis in the management of Wilms' tumor: a study by the

- United Kingdom Children's Cancer Study Group. *J Clin Oncol* 2002; 20(12):2768–2773.
25. Wilimas JA, Kaste SC, Kauffman WM, et al. Use of chest computed tomography in the staging of pediatric Wilms' tumor: interobserver variability and prognostic significance. *J Clin Oncol* 1997;15(7):2631–2635.
  26. Meisel JA, Guthrie KA, Breslow NE, et al. Significance and management of computed tomography detected pulmonary nodules: a report from the National Wilms Tumor Study Group. *Int J Radiat Oncol Biol Phys* 1999;44(3):579–585.
  27. Kodish E, Shina D, Morrison S, et al. Wilms' tumor with pulmonary nodules persisting after chemotherapy and radiation. *Med Pediatr Oncol* 1995;25(5):414–419.
  28. Shimmoto K, Ushigome S, Nikaido T, et al. Maturation of pulmonary metastases of Wilms' tumor after therapy: a case report. *Pediatr Hematol Oncol* 1991;8(2):147–157.
  29. Silvan AAM, del Castillo G, Caro AM, et al. Maturation of Wilms' tumor pulmonary metastases to benign fibromas after therapy. *Med Pediatr Oncol* 1984;12:218–220.
  30. Agress H Jr, Cooper BZ. Detection of clinically unexpected malignant and premalignant tumors with whole-body FDG PET: histopathologic comparison. *Radiology* 2004;230(2):417–422.
  31. Shulkin BL, Mitchell DS, Ungar DR, et al. Neoplasms in a pediatric population: 2-[F-18]-fluoro-2-deoxy-D-glucose PET studies. *Radiology* 1995; 194(2):495–500.
  32. Horwitz JR, Ritchey ML, Moksness J, et al. Renal salvage procedures in patients with synchronous bilateral Wilms' tumors: a report from the National Wilms' Tumor Study Group. *J Pediatr Surg* 1996;31(8):1020–1025.
  33. Sugawara Y, Zasadny KR, Grossman HB, et al. Germ cell tumor: differentiation of viable tumor, mature teratoma, and necrotic tissue with FDG PET and kinetic modeling. *Radiology* 1999;211(1):249–256.
  34. Wahl RL, Harney J, Hutchins G, et al. Imaging of renal cancer using positron emission tomography with 2-deoxy-2-(18F)-fluoro-D-glucose: pilot animal and human studies. *J Urol* 1991;146(6):1470–1474.
  35. Lowe LH, Isuani BH, Heller RM, et al. Pediatric renal masses: Wilms tumor and beyond. *Radiographics* 2000;20(6):1585–1603.
  36. Gyls-Morin V, Hoffer FA, Kozakewich H, et al. Wilms tumor and nephroblastomatosis: imaging characteristics at gadolinium-enhanced MR imaging. *Radiology* 1993;188(2):517–521.
  37. White KS, Kirks DR, Bove KE. Imaging of nephroblastomatosis: an overview. *Radiology* 1992;182(1):1–5.
  38. Antall PM, Myers MT, Dahms B, et al. Growth of a new intrarenal lesion in the remaining kidney of a patient with bilateral nephroblastomatosis and a previous nephrectomy for Wilms tumor. *Med Pediatr Oncol* 2000; 35(1):66–72.
  39. Rohrschneider WK, Weirich A, Rieden K, et al. US, CT and MR imaging characteristics of nephroblastomatosis. *Pediatr Radiol* 1998;28(6):435–443.